Applied Radiation and Isotopes 167 (2021) 109431

Contents lists available at ScienceDirect

Applied Radiation and Isotopes

journal homepage: http://www.elsevier.com/locate/apradiso

Qualification of the activities measured by gamma spectrometry on unitary items of intermediate-level radioactive waste from particle accelerators

Patrycja Dyrcz, Thomas Frosio *, Nabil Menaa, Matteo Magistris, Chris Theis

Radiation Protection Group, European Organization for Nuclear Research, 1211, Geneva 23, Switzerland

ARTICLE INFO

Keywords:
Intermediate-level radioactive waste
Heterogeneous source matrix
Gamma spectrometry qualification
Particle accelerators
Uncertainty quantification

ABSTRACT

In the frame of maintenance, upgrade and dismantling activities, activated equipment are removed from the accelerator complex and require characterization in view of their disposal as radioactive waste. The characterization process consists of a series of radiation measurements, complemented by analytical studies, which quantify the activity of radionuclides inside an object. A fraction of the radioactive waste produced at CERN presents contact dose-rates higher than 100 μSv/h, and can therefore be classified as LILW Waste ("Low and intermediate level radioactive waste"). These objects, due to the activation mechanisms, are often subject to large activity heterogeneities. The quantification of gamma-emitting radionuclides is typically performed by gamma spectrometry, under the assumption of homogeneous distributions of activity within an object. However, this assumption can lead to underestimating the activity value of such radionuclides. In this article we perform a gamma spectrometry qualification in order to quantify the impact of assuming homogenous distribution.

1. Introduction

In the frame of maintenance, upgrade and dismantling activities, activated equipment are removed from the accelerator complex and require characterization in view of their disposal as radioactive waste. A fraction of the radioactive waste produced at CERN presents contact dose-rates higher than 100 μSv/h, and can therefore be classified as LILW Waste ("Low and intermediate level radioactive waste"). The large majority of this radioactive waste is made of metallic compounds, without contamination.

In view of the elimination of LILW waste in the French national repository (ANDRA[1]), radiological characterization has to be performed in order to comply with ANDRA's acceptance criteria (ANDRA, 2018). These criteria require the estimation of the radiotoxicity levels, based on the radionuclide inventory. The radiological characterization of LILW waste has the purpose to establish the radionuclide inventory and the associated activity values of the candidate waste items (Zaffora et al., 2019; IAEA, 2009; ISO 21238, 2007; Zaffora, 2017). Gamma spectrometry techniques are commonly applied to estimate the activity of Easy-To-Measure nuclides (ETM) in waste. ETM (IAEA Nuclear Energy Series) are radionuclides which can be measured via non-destructive assay techniques (such as passive gamma spectrometry). Examples of ETM radionuclides are Co-60 or Na-22. These radionuclides have typically a Minimum Detectable Activity (MDA) which is below the ANDRA declaration thresholds for the counting times considered in the characterization process of LILW waste.

Qualification is a process used to evaluate the capacity of a model to predict physical quantities within a set of assumptions. This document describes the qualification of a measurement calibration of LILW waste. Due to their specific activation mechanisms in accelerator machines, LILW waste can have heterogeneous activation patterns. As shown in previous studies (Frosio et al., 2020), these heterogeneous matrices (subsequently denoted as "hot spot") can lead to underestimation of radionuclide activities.

In section 2, we provide an overview of the measurement setup and associated tools used to estimate ETM radionuclides activities. A description of the sample selected for measurement along with the reference geometry is available in sections 2.5. Sections 3 focuses on the uncertainties of the measured activities, due to waste geometry and heterogeneous source distribution.

2. Gamma spectrometry measurements

Evaluation of the gamma emitters' activities via gamma

* Corresponding author.
E-mail addresses: patrycja.kinga.dyrcz@cern.ch (P. Dyrcz), thomas.frosio@gmail.com (T. Frosio).
[1] Agence Nationale pour la gestion des Déchets RAdioactifs.

https://doi.org/10.1016/j.apradiso.2020.109431
Received 16 April 2020; Received in revised form 12 July 2020; Accepted 15 September 2020
Available online 22 September 2020

spectrometry is an important step of the characterizations of the LILW waste. Gamma spectrometry measurements are used to quantify the activity of gamma emitting radionuclides. The characteristics of the detectors used in this study and the tools for the efficiency calibration are described below.

2.1. Detectors characteristics

The gamma spectrometry measurements are performed in a dedicated area at CERN equipped with a High Purity Germanium detector (Falcon 5000 HPGe[2]) as shown in Fig. 1. The detector undergoes an on-site commissioning and a quality assurance program to verify continuous quality and reliability during the detector's use and operation.

2.2. In Situ Counting Object System (ISOCS)

ISOCS (In Situ Counting Object System) and LabSOCS (Laboratory Sourceless Calibration Software) from Mirion Technologies (Canberra) (Venkataraman et al., 2003) are applied in the laboratory for creating efficiency calibrations of good quality without using radioactive standards at the laboratory. The ISOCS software overcomes the limitations of traditional (tedious and expensive) efficiency calibration techniques and allows for practical modelling and accurate assay of almost any object in the laboratory. Previous attempts at simplified mathematical calibrations have had accuracy shortcomings due to assumptions that the detector was a point detector and due to limitations in accommodated sample shapes. With ISOCS, however, each individual detector has a unique set of characteristics that are experimentally validated and used to generate the efficiency calibrations. ISOCS/LabSOCS differ from the other available mathematical calibration packages in that a full factory characterization is performed on the detector. This process uses NIST-traceable sources and the well-known MCNP Monte Carlo modelling code. The diode MCNP Monte Carlo simulation model is determined by Mirion Technologies (Canberra) using NIST traceable radioactive sources.[3] The Monte Carlo model used in the ISOCS characterization is specifically validated, for the detector used in this study, for energies ranging from 50 keV to 1332 keV. The detector modelling uncertainties range from 5% at 50 keV to 3% at 1332 keV. The radiation response profile of each individual detector in free space (vacuum with no attenuation) is determined for a 1000 m diameter sphere around the detector covering an energy range of 10 keV through to 7 MeV. In the software, the characterized detector is selected from a list of available detectors – it then becomes incorporated into the model. At this point, the user needs to specify the sample geometry (i.e. the location and physical properties of the item being measured and the location and distribution of the source). The software does not require any additional information relating to the detector itself. This information is automatically extracted from a detector characterization file that is generated through the characterization process.

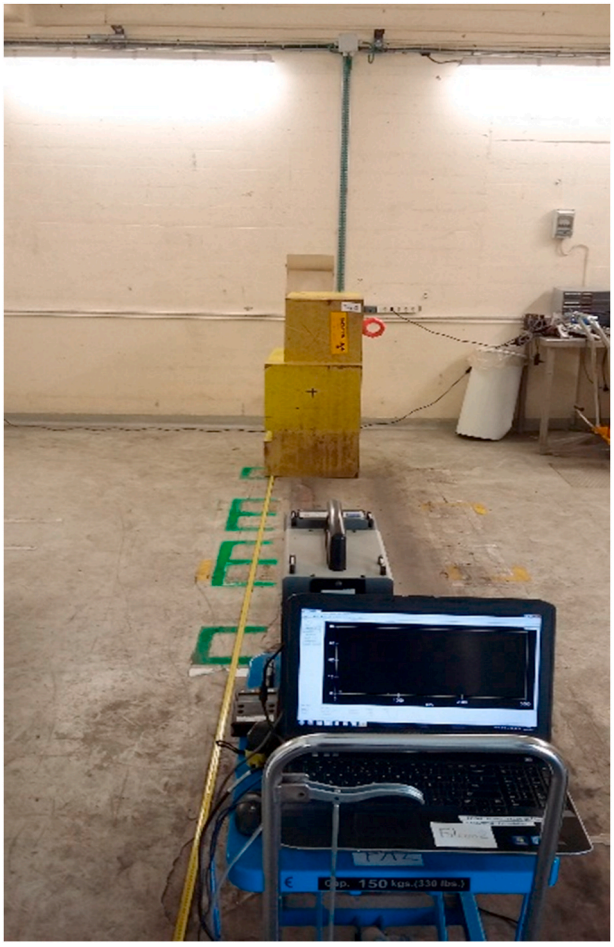

Fig. 1. Gamma spectrometry setup for in-situ measurement of waste.

The geometry description can be visualized and edited in the ISOCS/LabSOCS Geometry Composer application which contains a visualization interface of the sample geometry. The activity of a measured sample is given, as a function of efficiency calibration by Equation (1):

$$A = \frac{N_s(E)}{\varepsilon(E).\Delta t} \times \frac{1}{I_\gamma(E)} \quad (1)$$

Equation (1). Gamma spectrometry activity calculation.Where:

A is the activity of a certain radionuclide in the decay series;
$N_s(E)$ is the net peak area corresponding to energy E;
$\varepsilon(E)$ is the absolute full-energy peak efficiency corresponding to the geometry model at energy E;
$I_\gamma(E)$ is the emission intensity of photons with energy E;
Δt is the live time for collecting the spectrum.

Applying ISOCS Uncertainty Estimator (IUE) to create an ISOCS efficiency calibration, one needs to know the physical parameters of the object, such as dimensions or compositions of the container and sample. Some of those parameters are well known and do not vary appreciably. Other parameters are not-well-known, *e.g.*, the source distribution within the material matrix. These not well-known parameters contribute to the uncertainty of the calibration efficiency at each energy, and particularly at low energy as seen in the next. A tool called ISOCS Uncertainty Estimator (IUE) (Bosko et al., 2011; Spillane et al., 2010; Menaaet. al., 2011) has been developed by "Mirion Technologies (Canberra) Inc." to improve the quality of the gamma spectrometry uncertainty estimate. The user first runs the ISOCS software to compute the normal reference efficiency for the sample being measured. In our case, the reference model will be made of a uniform source distribution (no hot spot). For each not-well-known parameter, the user is required to provide an estimate of the parameter variation interval or values (in our case, by considering uniform distributions as we have no knowledge about hot spot variations); *e.g.*, by measuring a group of containers or consulting the manufacturer specifications for the containers or just by making educated guesses (also called expert elicitation). An example of

[2] http://www.canberra.com/fr/produits/hp_radioprotection/falcon-5000.asp.

[3] http://www.canberra.com/literature/isocs/application_notes/ISOCS-LabSOCS-App-Note-C39530.pdf.

these parameters in the IUE interface is provided in Fig. 2.

2.3. Guru framework

In order to fully exploit the efficiency calibration curves associated with the geometry parameters, we use the GURU (**G**eometry **U**ncertainty **R**eduction **U**tility) Data Analyzer framework (Frosio et al., 2020). For the sake of this study, it is needed to associate the model parameters with the efficiency values. When gamma spectrometry measurements are performed on samples, the knowledge of the geometry description, including dimensions, position with respect to the detector, material composition, and relative activity concentration is often not well known, especially for the two last parameters. GURU offers a framework and methodology to identify the best models that better describes the "actual" Geometry, based on combining the different gamma spectrometry results.

A large set of geometry models is generated using IUE, based on the knowledge we have of a sample. By varying the geometry, we produce a set of perturbed efficiency calibration curves. These curves are used to evaluate activity results as a function of the geometry.

GURU makes use of the FOMs (Figure of Merits) that rely on the multi-count and line activities consistencies. Multi-count consistency is a constraint assumption in which detector measurements performed at different locations of a sample should give the same activity results, if the entire object is measured. Additionally, multi-line consistency is a constraint assumption in which, the different line activity results of a radionuclide should be consistent. These constraints are used within the GURU framework based on the FOM presented in Equation (2):

$$FOM_i(j) = \sum_k \left(A_i^k(j) - A_i(j)\right)^2 \quad (2)$$

Equation (2): Partial FOM of a gamma line emission for a gamma emission j and a perturbed geometry model j.Where:

$A_i(j)$ is the average over the K detectors of the activity for the gamma emission j in the geometry model i,
$A_i^k(j)$ is the activity calculated for the radionuclide associated to the emission j in the model i with the detector k.

Each partial $FOM_i(j)$ is associated to a partial rank. These ranks are summed over the gamma emissions j in order to get a final rank which depends only on the geometry model. The best-estimate geometry model is the one with the lowest rank, which means it has the lowest FOM.

2.4. Reference geometry for efficiency calibration

The characteristics of the reference geometry are shown in Table 1 and the corresponding ISOCS/LabSOCS geometry parameters are shown in Fig. 3.

To generate the reference ISOCS calibration curve, one needs to know the physical parameters, such as the dimensions of the item, and the material composition. The model based on these reference parameters will be denoted as the reference model or uniform model in the next parts of this document.

Table 1
The characteristics of the reference ISOCS model.

The item dimensions [cm]	50 × 80.5 × 106 cm^3
The item mass [kg]	2650 kg
Material composition of the item	iron: 100.00%

The detector-to-source (item) distance is set to the actual counting distance (face 1 and face 2 are set to 320 cm, face 3 is set to 53 cm while face 4 is set to 200 cm, the differences in distance arise from retaining the dead time of the detector below 10%). The material density is set at 6.21 g/cm^3.

2.5. Setup and sample description

Evaluation of the gamma emitters' activities via gamma spec is an important step of the characterizations of the LILW waste. This type of waste is characterized by a heterogeneous activity distribution and therefore it represents an excellent example of the application of the methodology presented in this paper. In order to assess the impact of considering or ignoring the activity distribution, we performed tests with a unitary piece made of iron, which we measured with a HPGe Falcon 5000 detector. Fig. 4 shows the measured unitary piece with its dimensions.

Measurements are performed for the four faces of the unitary piece, as indicated in Fig. 5, and the results are given in Table 2. The maximum dose rate at contact identified on the unitary piece reaches 400 μSv/h (for face 1) and the minimum is 9 μSv/h (for face 3). The source-to-detector distance is selected in order to have a maximum allowed dead-time of 10% and the measurement time ranges from 10 000 to 75 000 s.

The results of the four gamma spectrometry measurements with reference model are presented in Table 3. For these measurements, we produce a set of efficiency calibration curves for each face, using the "complex box" ISOCS geometry template. We consider a uniform source distribution in the material matrix and an envelope geometry, neglecting the recess of the top part (see Fig. 4). An illustration of the performed measurements on all the item faces is shown in Fig. 5. These assumptions will be discussed in the next section 3.1 concerning the geometry envelop and section 3.2, regarding the uniform source distribution.

As it can be seen in Table 3, the activity values obtained with the reference model show high ratios between the four measurements. The ratio of highest and lowest activities between the two opposite faces assuming the uniform source distribution gives an estimate of the relative activity concentration variation range of the hot spots. In the next section, we call this parameter the "contrast". The uncertainties given in

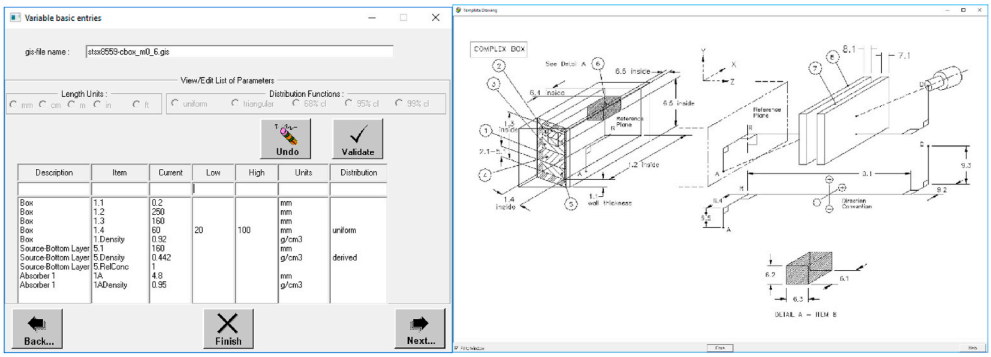

Fig. 2. Typical IUE data input screen. Parameters are entered here to describe the amount and type of variation for the geometry model.

Edit dimensions - Boite Complexe

Description:
Comment:
Units: mm cm m in ft

OK
Cancel
Apply
Help
View Drawing...

No.	Description	d.1	d.2	d.3	d.4	d.5	d.6	Material	Density	Rel. Conc.
1	Boite	0.0001	500	1060	805			dryair	0.00129	
2	Source - Couche	0						(none)	0	0.00
3	Source - Couche 2	0							0	0.00
4	Source - Couche 3	0							0	0.00
5	Source - Couche	1060						iron	6.2112	1.00
6	Source - Source							iron	6.2112	1.00
7	Absorber 1	0							0	
8	Absorber 2	0							0	
9	Source-Detector	3200	0	0	0	0				

Fig. 3. Efficiency calibration geometry parameters for the reference model using the Complex Box template.

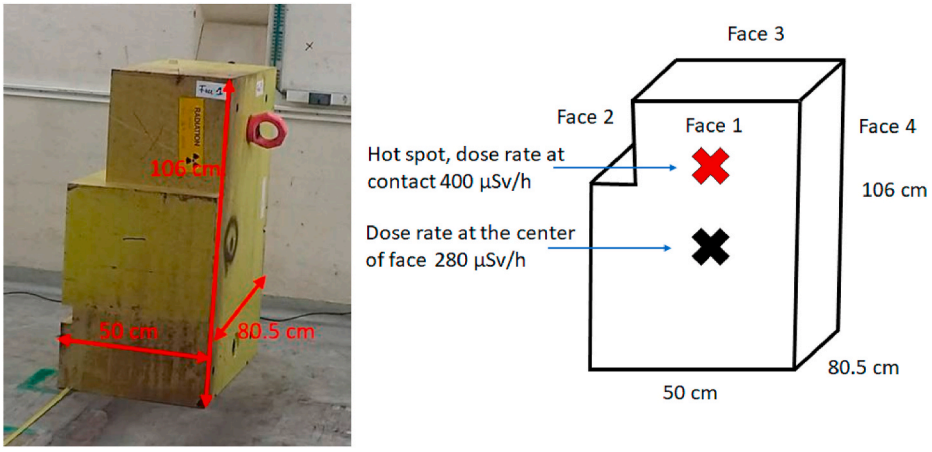

Fig. 4. Candidate LILW unitary iron piece. Faces are identified on the right schematic view.

Table 3 are the uncertainties reported by GENIE2K. They include nuclear data (such as half-lives and emission rate) and mathematical efficiency calculation uncertainties.

These contrasts demonstrate the heterogeneous distribution of activities between faces 1 and 3 or 2 and 4. Moreover, the high value of these ratios originate mainly from the activity heterogeneities in the waste matrix observed by measuring the dose rate on each face. The measurement of one single face with the assumption of a uniform source distribution is clearly inadequate to properly model the waste and compute the ISOCS efficiency calibrations.

Performing an accurate gamma spectrometry on objects with high contrasts is challenging and needs precautions. As a consequence, section 3.2 focuses on the matrix heterogeneities impact on the activity results.

3. Qualification of the activities for the unitary piece

3.1. Impact of the envelop geometry

The shape of the iron unitary piece is not regular. Hence, it is not possible to implement the actual geometry of this unitary piece into the IUE calculations. A box geometry is assumed to represent the item. Thus, we perform calculations to investigate the influence of different geometry configurations on the activity results. Two geometry models are considered. The first model assumes the maximum dimensions (maximum envelop) of the iron block are $50 \times 80.5 \times 106$ cm^3. In the second approach, we assume a smaller (or minimum) envelop volume whose dimensions are limited by the dimensions of the top part of the item (see Fig. 4) giving a volume of $45 \times 75.5 \times 106$ cm^3. Moreover, both geometry models have homogeneous source distributions. The ratios of the activity results of the two considered models (maximum/minimum) vary between 0.93 and 0.94 for energies ranging from 60 keV to 3 MeV. We conclude that the maximum envelop model overestimates the activities by about 6%, the rest of this study uses the maximum envelop geometry model as the reference model.

3.2. Matrix heterogeneity impact: source distribution

In section 2.5, we showed that the heterogeneous source distribution in the matrix has a high impact on the gamma spectrometry results. Note that LILW waste can have large source heterogeneities and they have to be studied and considered for an accurate characterization. Hence, we target to study two different aspects:

- First, we want to assess the best-estimate of the "real" activity value within the waste item. For this purpose, we perform the GURU optimization of the efficiency calibration models in order to compare the uniform model activities to the optimized models.
- Then, we want to quantify the uncertainties originating from the uniform model assumption, on the activity values. By the quantification of uncertainties, we are able to construct correction factors applied to the activity values. Hence, we calculate a reasonably large envelop value for the activity results measured with the reference model. This approach has the benefit to simplify the operational procedure during the LILW waste characterization process.

The mathematical framework of this qualification process for gamma spectrometry results is detailed in next section 3.3.

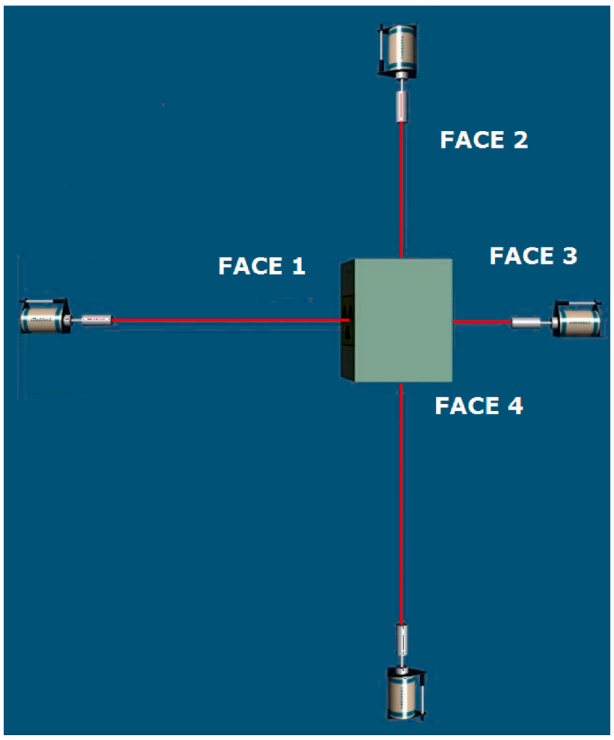

Fig. 5. Geometry models for four faces of the sample analyzed in this document.

3.3. Approach to qualify activity values

The qualification is a process used to evaluate the capacity of a model to predict physical quantities within a set of assumptions. The aim is to quantify random errors and biases of a reference model. It is generally achieved by comparing this reference model with an optimized (experimental) model which represents the best knowledge we can have regarding a system.

Mathematically, as a first step we evaluate the best-estimate of the "real" activity value (red line in Fig. 6), with the knowledge of the reference model (uniform source distribution, blue line in Fig. 6).

As a second step, based on the large set of perturbed geometry models (generated with IUE) with the Probability Density Function (PDF) shown in Fig. 6, we construct a correction factor $(1 + \mathrm{CF}(\mathrm{E}))$ to apply to the reference model and to get an envelope activity value. This envelop value is identified with a confidence level of 97.5% (kσ, yellow line in Fig. 6). The uncertainty is represented by a systematic error (bias $\mathbb{B}$) and a random error (standard deviation σ) (GUM, 2008a) (GUM, 2008b) that we construct with a confidence level of 97.5%.

Hence, the value of correlation factor $1 + \mathrm{CF(E)}$ is determined in Equation (3), where $\mathrm{CF}(\mathrm{E}) = \mathbb{B} + k\sigma$ in relative values, $A_0(E)$ is the activity of the reference model and $A_p(E)$ is the activity of the envelop model.

$$A_0(E)\ (1 + \mathrm{CF(E)}) = A_p(E) \tag{3}$$

Equation (3): Relation between reference model activity value and envelop value constructed with a confidence level of 97.5%

Note that the correction factor can be negative, if the expectation value (i.e. the mean of the optimized models with hot spots) is below the reference model's activity value. In such a case, the envelop activity value is assumed to be equal to the reference model value. If the accurate source distribution is unknown, then the optimized value calculated with GURU will serve as the best-estimate of the "real value" and it will subsequently be referred to as such.

The actual "real value" (red curve) is not necessarily on the left side of the expectation value and can be located in the whole statistical distribution.

We now consider the average of the activity results of two detectors facing each other from opposite sides of the object as presented in Equation (4).

$$\left(A_0^1(E) + A_0^2(E)\right)(1 + \mathrm{CF(E)}) = \left(A_p^1(E) + A_p^2(E)\right) \tag{4}$$

Equation (4): Relation between reference model average activity value and detector average envelop value.Where:

$A_p^1(E)$ and $A_p^2(E)$ respectively represent the activities calculated at energy E for detector 1 and 2 *using the envelop geometry model p*. The notation is similar for $A_0^1(E)$ and $A_0^2(E)$ with reference model

Activity $A_p^1(E)$ can be expressed by Equation (1), and we are considering the ratio of efficiency calibration values of two opposite detectors. The correction factor is presented in Equation (5), where $\varepsilon_p^1(E)$ and $\varepsilon_p^2(E)$ represent respectively the efficiency calibration calculated at energy E for detector 1 and 2 in the envelop geometry model p. The notation is similar for $\varepsilon_0^1(E)$ and $\varepsilon_0^2(E)$ with the reference model. The quantity $R(E) = \frac{A_0^2(E)}{A_0^1(E)}$ is the activity ratio of the two detectors results obtained with the reference model.

Table 2
Main acquisition parameters of the gamma spectrometry measurements for the four faces of the iron unitary piece. The hot spot dose rate value at contact of the item is 400 μSv/h. The minimum dose rate value at contact is 9 μSv/h.

FACE	Distance [m]	Dead time	Live measurement time [s]	Dose rate at the center of each face at contact [μSv/h]	Dose rate at the detector [μSv/h]
1	3.2	5%	10000	280	2
2	3.2	4.1%	10000	96.5	1.5
3	0.53	7.5%	50000	10	2.5
4	2	9.8%	72000	132	4.7

Table 3
List of identified radionuclides with their activities (relative uncertainties) for the four faces of the unitary piece. Values found below the MDA are neglected in this study. The uncertainties are quoted at 1σ. The geometry model uncertainties are not included. The mass of the item is 2650 kg.

FACE	Co-60 [Bq/g]	Na-22 [Bq/g]	Sc-44<Ti-44 [Bq/g]	K-42<Ar-42 [Bq/g]
1	2.48E+02 (5%)	4.83E-01 (10%)	8.49E+00 (6.2%)	1.22E+00 (9.5%)
2	1.09E+02 (5%)	< MDA	5.89E-01 (11%)	8.08E-02 (29%)
3	1.62E+01 (5%)	3.96E-03 (21%)	2.86E-02 (8.5%)	< MDA
4	1.41E+02 (5%)	1.15E-01 (7.5%)	1.60E+00 (6%)	2.29E-01 (9%)
Contrast between faces 1 and 3	16	122	297	Not Applicable
Contrast between faces 2 and 4	1.3	Not Applicable	3	3

$$(1+\mathrm{CF(E)}) = \frac{\left(A_p^1(E)+A_p^2(E)\right)}{\left(A_0^1(E)+A_0^2(E)\right)} = \frac{\left(A_0^1(E)\frac{\varepsilon_0^1(E)}{\varepsilon_p^1(E)}+A_0^2(E)\frac{\varepsilon_0^2(E)}{\varepsilon_p^2(E)}\right)}{\left(A_0^1(E)+A_0^2(E)\right)} = \frac{\left(\frac{\varepsilon_0^1(E)}{\varepsilon_p^1(E)}+R(E)\frac{\varepsilon_0^2(E)}{\varepsilon_p^2(E)}\right)}{(1+R(E))} \quad (5)$$

Equation (5): Expression of the correction factor for the average activity values over two detectors.

3.4. Optimization of geometry models

A set of ISOCS geometry models are constructed using IUE in order to vary the hot spots locations, dimensions, number and relative source concentrations. The location and dimension of the hot spots are allowed to vary in the entire matrix layers with a number of hot spots varying from 1 to 10. The contrast varies between 1 and 400 to represent the observed distribution activity ratio from Table 3 between the two opposite faces.

The distribution of efficiency calibration curves is studied for each detector face and summarized in Fig. 7. One can see that an important bias of −85% is observed compared to the reference model and the standard deviation is around 15% at 45 keV. When energy increases, the bias is reduced to 50% at 3 MeV. Considering the measurement on each face independently, one would suggest that the most appropriate envelop value could have a relative difference to the reference model of −99.64% even at energies above 2 MeV. Hence, as the activity is inversely proportional to the efficiency (see Equation (1)), the envelop activity value would be around 300 times higher than the reference efficiency for the same range of energies. From a practical point of view, these results confirm that measuring only one face of a heterogeneous item can lead to not detecting a radionuclide that is otherwise present and detectable on another face, as in the case of Na-22 in faces 2 and 1 of the sample unit.

The efficiency calibration optimization is performed with GURU using multi-count consistency figure of merit FOM. The activity values of the whole set of models are plotted in Appendix A, Fig. 11. The radionuclides Co-60 and Sc-44<Ti-44 are represented with different ranges of relative activity concentrations for each set of opposite measurement faces. The area where the two curves cross each other represents the "best" optimized models according to the best knowledge we have of the waste item. The activity ratio of the uniform activity distribution and optimized models are presented in Table 4. One can see that after optimization, the ratio becomes very close to 1, showing the usefulness and effectiveness of the methodology. The highest ratios are found between face 1 and 3 which have the highest dose rate ratio. The data are illustrated in Fig. 8.

The optimization process allows for assessing the best-estimate activity result to the real value (red line, Fig. 6). Table 5 below presents the average activity values for the uniform and optimized models over two opposite faces.

Since the optimization is performed over two faces at a time, we opted for averaging the results obtained for each pair of faces. Uncertainties on the two faces average is calculated as the quadratic sum of single faces uncertainties. Hence, averaging increases the final uncertainty of the measurement. This approach was followed for both the reference and the optimization model activity results. Averaging over two opposite faces allows for experimentally observing a ratio from 0.73 to 2.8 (see Table 5). Even though the dose rate values show a factor of ~28 (between faces 1 and 3) and a factor of ~0.7 (between faces 2 and 4), the difference of the activity values between the uniform and the optimized models is of the order of a factor of 2. Moreover, taking the average of the activity values between the four faces, leads to a factor difference between the uniform and optimized models of ~1.5. Hence, for applications where an activity uncertainty of ~50% is tolerated, averaging the activities obtained using the reference model leads to reasonable results. The study shows also that, the difference of the activity values between the average of the optimized results of the two faces and the four faces is 17%. The correction factor depends on the source contrast and on the gamma ray emission energies of the radionuclides of interest. Using multiple detectors over multiple faces at a time could greatly improve the knowledge of hot spot locations, dimensions and concentrations to reach an efficiency close to tomography reconstruction (Carrelet al., 2014) (Dumazertet al., 1613).

3.5. Envelop model selection

The qualification method, as described in section 3.3 is applied, considering different contrast values and different energies from 45 keV to 3 MeV. We generate efficiency calibration curves with IUE and we consider Equation (5) to compute a set of "envelop" correction factors "CF". For the sake of illustration, Fig. 9 presents the results obtained for Co-60 and Sc < Ti-44 between face 1 and 3. The corresponding contrasts selected are based on the activity ratio that we obtain from the gamma

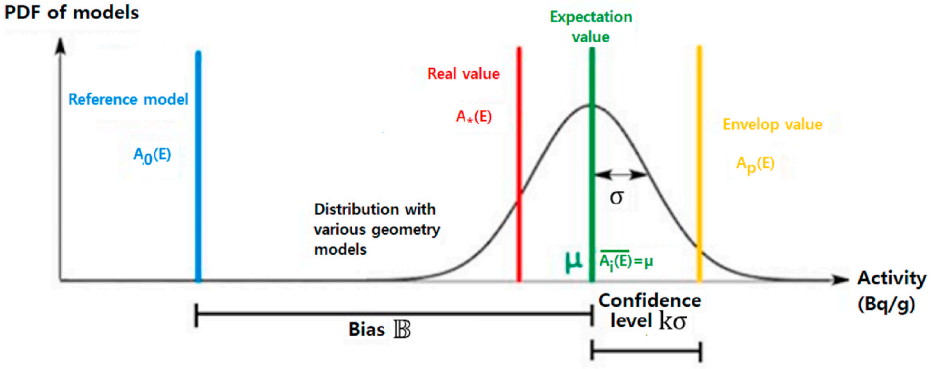

Fig. 6. Schematic representation of the parameters involved in the qualification process.

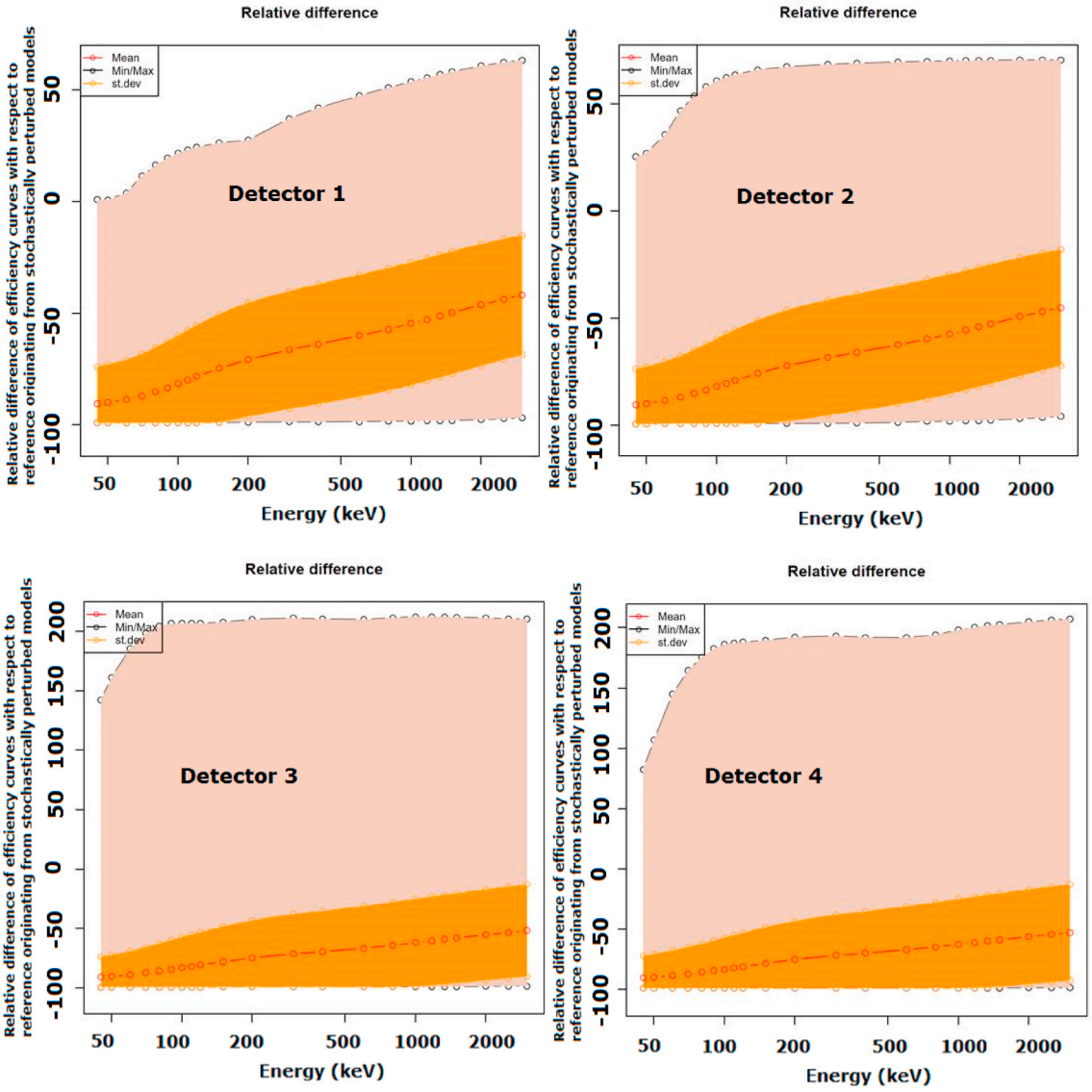

Fig. 7. Relative efficiency difference (%) as a function of energy compared to the reference model. The brown envelope presents the range of efficiency variations. The orange envelope describes the range of variations around the expectation value (red curve) at 1 σ. (For interpretation of the references to colour in this figure legend, the reader is referred to the Web version of this article.)

spectrometry measurements, with a uniform source distribution within the material matrix (see Table 3).

Fig. 9 shows that the ratio between the "best estimate" value and the uniform value is of 0.8 for Sc < Ti-44. The expectation value of the ratio with respect to the reference model (bias without any random uncertainty) is of 13.65 and the envelop CF value is 73.57. The considered contrast ranges from 1 to 400 as it can be seen in Table 3 with a ratio of activities between face 1 and 3 of 297 in the case of uniform source distribution.

Regarding Co-60, we consider a contrast ranging from 1 to 25 (the ratio of activities between faces 1 and 3 is around 16 for the uniform source distribution model). The "best estimate" value reaches a ratio of 1.8 compared to the reference model. The envelop value's ratio with the uniform model is of 7.05 for this situation.

One can see in Fig. 9 that the cases of Co-60 and Sc < Ti-44 present strong differences. First of all, the highest contrast for Sc < Ti-44 induces a spread of the probability distribution (histogram) as the hot spots can have an activity concentration up to 400 times higher than the rest of the matrix. This leads to ratios from 1 to 150 between the uniform and optimized model. At the opposite, for Co-60, the contrast ranges from 1 to 25 leading to a maximum ratio between perturbed models and uniform model of 10.

Note that the optimized activity value is below a factor of 2 compared to the uniform activity distribution value for both radionuclides. This result is not necessarily expected as the activities from the perturbed models vary from a factor of 10–150 for Co-60 and Sc < Ti-44 compared to the uniform model. This shows that, even despite the

Table 4
Activity and dose rate ratio for faces 1 and 3, and for faces 2 and 4. Uncertainties are given at 1σ.

	UNIFORM		OPTIMIZED	
	Faces 1 and 3	Faces 2 and 4	Faces 1 and 3	Faces 2 and 4
Co-60	16 ± 1	0.8 ± 0.05	1.0 ± 0.07	1.0 ± 0.07
Na-22	122 ± 29	N/A	1.0 ± 0.24	N/A
Sc < Ti-44	297 ± 32	0.4 ± 0.05	1.1 ± 0.12	1.0 ± 0.12
K < Ar-42	N/A	0.4 ± 0.11	N/A	1.0 ± 0.30
Dose rate at contact face center	28	0.7	N/A	N/A

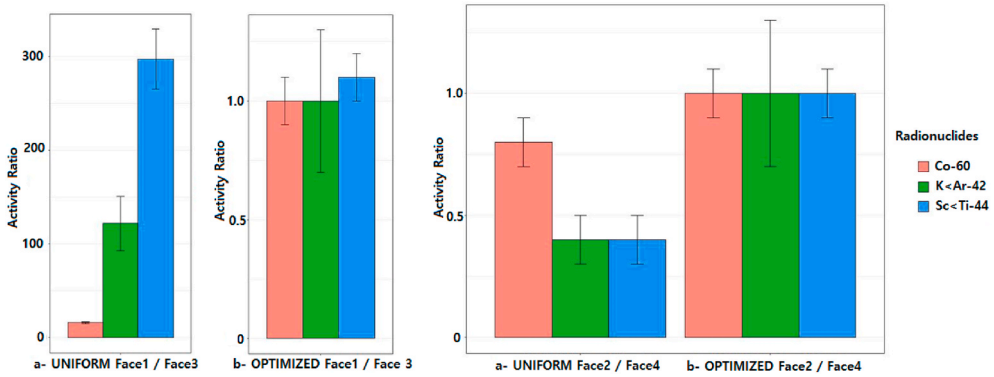

Fig. 8. Activity ratio for pair of detectors faces 1 and 3 and faces 2 and 4 before and after geometry optimization.

Table 5
Average activity over the two opposite faces with uniform and optimized models. Uncertainties are given at 1σ. Note that the uniform activity result uncertainties do not take into account the geometry model uncertainty due to the ill-defined parameters.

	UNIFORM		OPTIMIZED		Ratio OPTIMIZED/UNIFORM	
	Faces 1 and 3	Faces 2 and 4	Faces 1 and 3	Faces 2 and 4	Faces 1 and 3	Faces 2 and 4
Co-60 [Bq/g]	1.35E+02 ± 5%	1.25E+02 ± 4%	2.49E+02 ± 4%	1.32E+02 ± 4%	1.84 ± 0.11	1.06 ± 0.05
Na-22 [Bq/g]	2.43E-01 ± 10%	< MDA	1.79E-01 ± 12%	N/A	0.73 ± 0.11	N/A
Sc < Ti-44 [Bq/g]	4.23E+00 ± 6%	1.09E+00 ± 5%	3.52E+00 ± 5%	3.06E+00 ± 6%	0.83 ± 0.07	2.8 ± 0.23
K < Ar-42 [Bq/g]	< MDA	1.55E-01 ± 10%	N/A	2.59E-01 ± 15%	N/A	1.67 ± 0.3

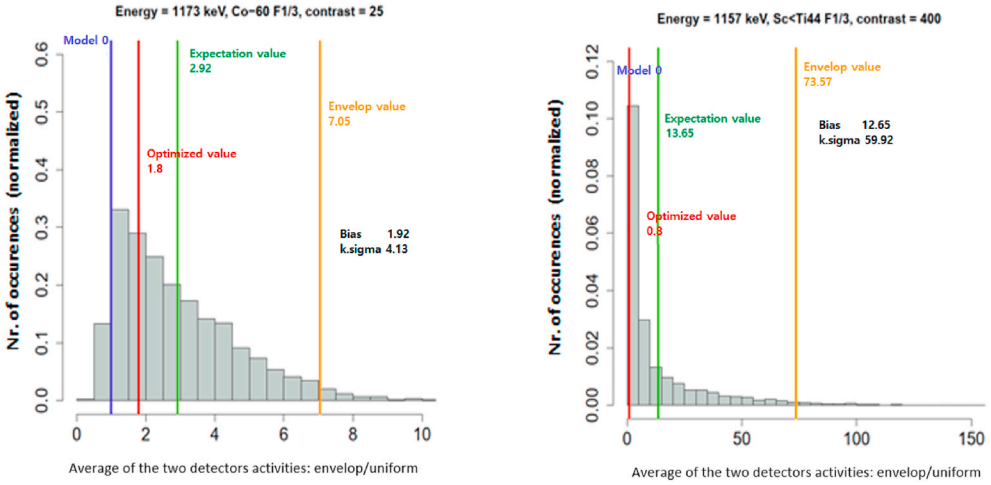

Fig. 9. Distribution of correction factors (1 + CF(E)) normalized for the uniform distribution (reference model, blue line). Optimized value is represented by the red line, expectation value is represented by the green line and characterizes the bias due to a heterogeneous source distribution ($\mathbb{B} = \boldsymbol{expectation\_value} - 1$). The envelop value is represented by the orange line and characterizes the random uncertainty due to a heterogeneous source distribution ($\boldsymbol{k\sigma} = \boldsymbol{penalizing\_value} - \mathbb{B}$). (For interpretation of the references to colour in this figure legend, the reader is referred to the Web version of this article.)

activity ratio of 297 (Sc < Ti-44) and 16 (Co-60) between the uniform model of faces 1 and 3, the contrast seems to be overestimated.

The best optimized models have most of the matrix with similar source concentration: either because the hot spots are small and therefore most of the matrix is homogenous, or because the hot spots are very large and therefore they represent a large fraction of the matrix.

We calculate the geometric centre C of the hot spots weighted by their corresponding relative source concentrations for the best models, as described in Equation (6), in order to estimate the best models contrasts. In particular, V_i is the volume of the hot spot i having the relative source concentration S_i, and V_T is the total volume of the waste item.

We consider that this calculation is an acceptable estimate of the contrast a posteriori of the optimization.

$$C = \frac{1}{V_T}\frac{\sum_i V_i S_i}{\sum_i S_i} \tag{6}$$

Equation (6). Geometric centre of hot spots weighted by source concentration.

For Co-60, the results show that the contrasts of the best estimate models range from 2 to 6 when calculated with Equation (6), instead of the 16 observed by the activity ratio between face 1 and 3 with the uniform model. For Sc < Ti-44, the contrasts of the best estimate models range from 5 to 15 (Equation (6)) instead of 297 as observed by the activity ratio between face 1 and 3 with the uniform model.

In both cases, we can conclude that the contrast, in the item, is not as high as predicted by the ratio of activity values measured with uniform distribution.

The energy dependence and the source distribution contrast of the correction factor is illustrated in Appendix B, Fig. 12. We observe that the contrast is the most impacting parameter and the correction factor increases with the contrast. Hence, this parameter has to be well quantified to avoid over penalization of the activity results. The

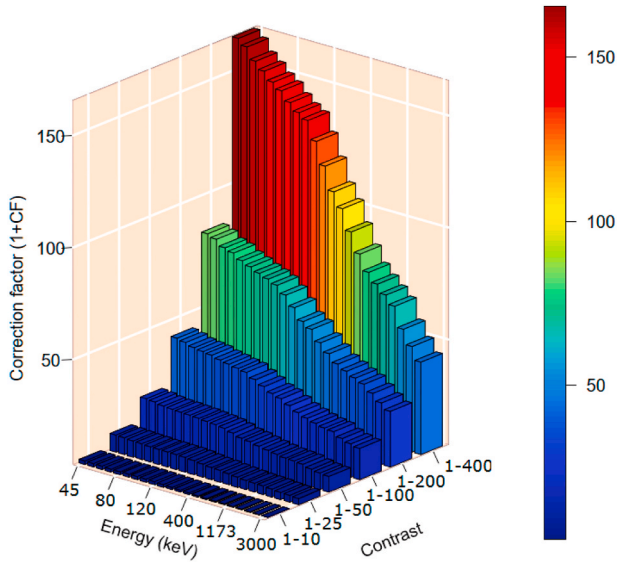

Fig. 10. Envelop correction factors for the LILW waste studied in this document as a function of energy and source distribution contrast ranges.

Table 6
Envelop correction factors (1 + CF(E)) to consider as a function of energy and source distribution contrasts.

Energy (keV)	[[1-10]	[1–25]	[1–50]	[1–100]	[1–200]	[1–400]
45	4.7	10.6	21.3	42.8	83.9	165.6
50	4.6	10.6	21.0	42.0	82.5	162.9
60	4.5	10.3	20.3	40.8	79.8	157.7
70	4.5	10.1	19.9	40.2	78.7	154.3
80	4.4	10.0	19.8	39.6	76.3	150.5
90	4.4	9.8	19.6	38.6	74.7	147.8
100	4.4	9.8	19.3	37.9	72.8	143.6
110	4.4	9.8	19.0	37.1	71.5	140.2
120	4.3	9.7	18.6	36.4	69.8	137.8
150	4.2	9.4	18.1	34.4	66.5	129.6
200	4.1	8.9	17.2	32.4	62.0	119.7
300	3.9	8.5	16.0	30.3	57.0	109.3
400	3.8	8.3	15.5	29.2	54.6	102.9
600	3.7	7.9	14.7	27.2	49.7	93.6
800	3.6	7.6	13.9	25.2	45.9	84.8
1000	3.5	7.3	13.2	23.8	42.4	77.8
1173	3.5	7.1	12.7	22.6	40.3	73.6
1332	3.4	6.9	12.5	21.7	38.4	69.9
1500	3.3	6.7	12.2	21.1	36.8	66.0
2000	3.2	6.4	11.2	19.2	33.8	56.8
2500	3.2	6.1	10.5	17.9	30.6	50.2
3000	3.1	5.9	10.1	17.0	28.0	44.4

correction factor increases when the energy decreases due to the attenuation in the material leading to lower efficiency values. Fig. 10 shows the (1 +CF(E)) "envelop" values with different ranges of contrast and energies from 45 keV to 3 MeV. For energies corresponding to main gamma emitters, like Co-60 identified in waste item and high source contrasts, the correction factor can be of order of 70. This means that the activity of Co-60 computed for 1173 keV and 1332 keV could be underestimated by a factor of 70 with a reference model.

Table 6 summarizes the data presented in Fig. 10.

In order to be conservative with a confidence level 97.5% we apply the envelop correction factor. The correction factor is valid for comparable shape and activity distributions of the waste items.

Hence, we strongly recommend performing multiple detector measurements on which the average will be calculated including the most radioactive faces, using a reference model.

Table 7 and Table 8 present activities for all identified radionuclides before and after optimization.

4. Conclusions

This study demonstrates a novel qualification methodology to estimate the ETM activity results of an LILW waste item based on gamma spectrometry technique. The waste item is characterized with a high source distribution heterogeneity of the matrix material. In order to estimate the impact of this source distribution contrast on the activity results, geometry models are simulated by varying the hot spots dimensions, locations, and source relative concentrations. From this set of geometry models, an uncertainty analysis is performed. The study presents also the geometry optimization results that allows for selecting the optimized (best) models taking into account the FOM (Figure of Merit) that rely on the multi-count and line activities consistencies (Frosio et al., 2020).

The main objective of the method is to reduce the over-estimation of activity by improving the measurement precision. Hence, a better estimation of the waste radiotoxicity can be performed for waste storage purposes and management costs.

The variation of the sample's geometry dimensions presents a small impact compared to the variation of the activity distribution. As shown in Section 3.1, the impact of the envelop geometry model is negligible, as the uncertainty is about 6%.

The uncertainty analysis shows that using one detector spectrometry measurement induces high activity results uncertainties due to the activity heterogeneity of the waste item. For LILW waste characterization, this study recommends using detector average results of multiple faces rather than limiting to one side gamma spectrometry measurement.

The geometry optimization using GURU framework and methodology allowed estimating the best-known activity results. Even though the dose rate values show a factor of ~28 (between faces 1 and 3) and a factor of ~0.7 (between faces 2 and 4), the activity values difference between the uniform and the optimized models is of the order of a factor of 2. Moreover, taking the average of the activity values between the four faces, leads to a factor difference between the uniform and optimized models of ~1.5 even with contrast values as high as 400. Yet, the validity of extrapolating this result with notably higher ratios would have to be studied further. The study shows also that the difference of the activity values between the average of the optimized results of the two faces and the four faces is 17%.

The optimization results show that the ratio of the two detectors activities using the reference models does not accurately represent the actual contrast of the item. On the other hand, the geometry optimization allows defining the best-known contrast distribution or the activity contrasts within the waste item.

We have shown, by comparison with an optimized model that, performing measurement in the following conditions lead to reasonably conservative results:

Table 7
Activity values for radionuclides measured in faces 1 and 3. The uncertainties are quoted at 1σ. The geometry model uncertainties are not included.

	Co-60 (1173 keV) [Bq/g]	Co-60 (1332 keV) [Bq/g]	Na-22 (1274.5 keV) [Bq/g]	Sc < Ti-44 (1157 keV) [Bq/g]
Optimized - average over faces 1 and 3	2.47E+02 ± 4%	2.52E+02 ± 4%	1.79E-01 ± 12%	3.54E+00 ± 5%
Uniform face 1	2.57E+02 ± 6%	2.53E+02 ± 6%	4.83E-01 ± 10%	8.49E+00 ± 6%
Uniform face 3	1.62E+01 ± 6%	1.62E+01 ± 6%	3.96E-03 ± 21%	2.86E-02 ± 8%
Uniform - average over faces 1 and 3	1.37E+02 ± 6%	1.35E+02 ± 6%	2.43E-01 ± 10%	4.23E+00 ± 6%

Table 8
Activity values for radionuclides measured in faces 2 and 4. The uncertainties are quoted at 1σ. The geometry model uncertainties are not included.

	Co-60 (1173.2 keV) [Bq/g]	Co-60 (1332.5 keV) [Bq/g]	Sc < Ti-44 (1157 keV) [Bq/g]	K < Ar-42 (1524.7 keV) [Bq/g]
Optimized - average over faces 2 and 4	1.32E+02 ± 4%	1.33E+02 ± 4%	3.06E+00 ± 6%	2.59E-01 ± 15%
Uniform face 2	1.09E+02 ± 6%	1.09E+02 ± 6%	5.89E-01 ± 11%	8.08E-02 ± 29%
Uniform face 4	1.40E+02 ± 6%	1.40E+02 ± 6%	1.60E+00 ± 6%	2.29E+00 ± 9%
Uniform - average over faces 2 and 4	1.25E+02 ± 9%	1.25E+02 ± 9%	1.09E+00 ± 5%	1.55E-01 ± 10%

- Perform multiple detector measurements,
- Compute the average of activity results for the most radioactive faces of the sample,
- Consider the reference model.

Declaration of competing interest

The authors declare that they have no known competing financial interests or personal relationships that could have appeared to influence the work reported in this paper.

Appendix A

Activities calculated for different radionuclides, different relative source concentration ranges and two opposite faces measured.

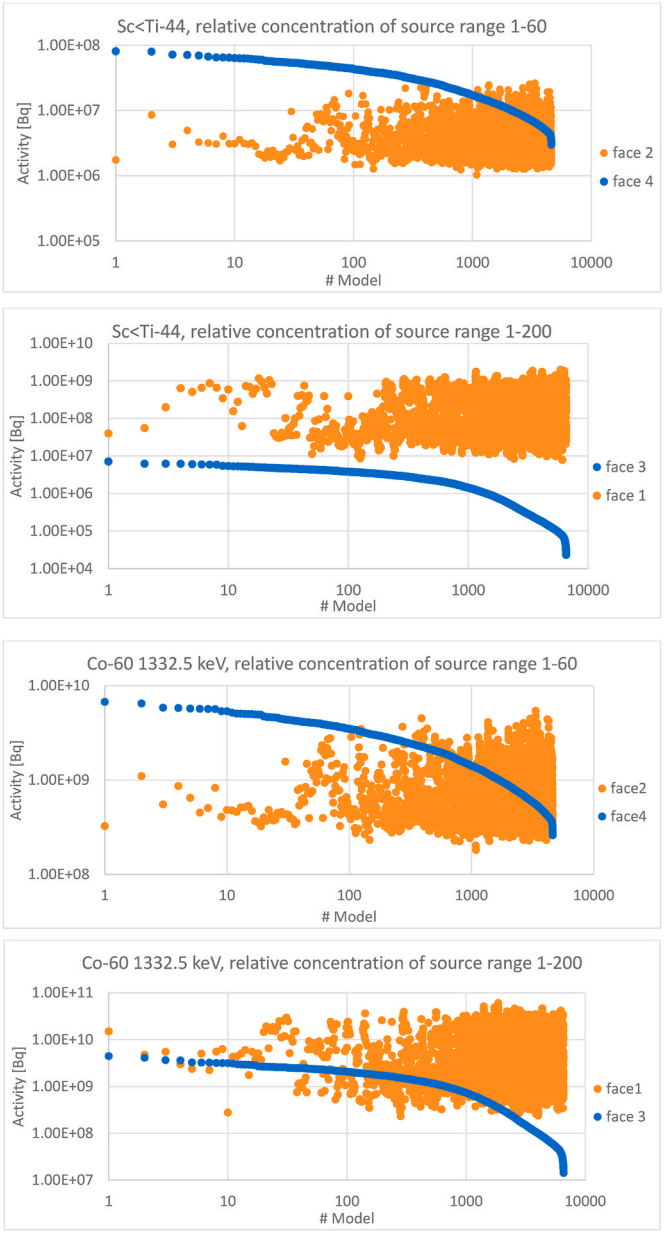

Fig. 11. Activities for different radionuclides for opposite faces. Source distribution contrasts are 60 and 200.

Appendix B

Illustration of the activity values dependency in energy and contrast.

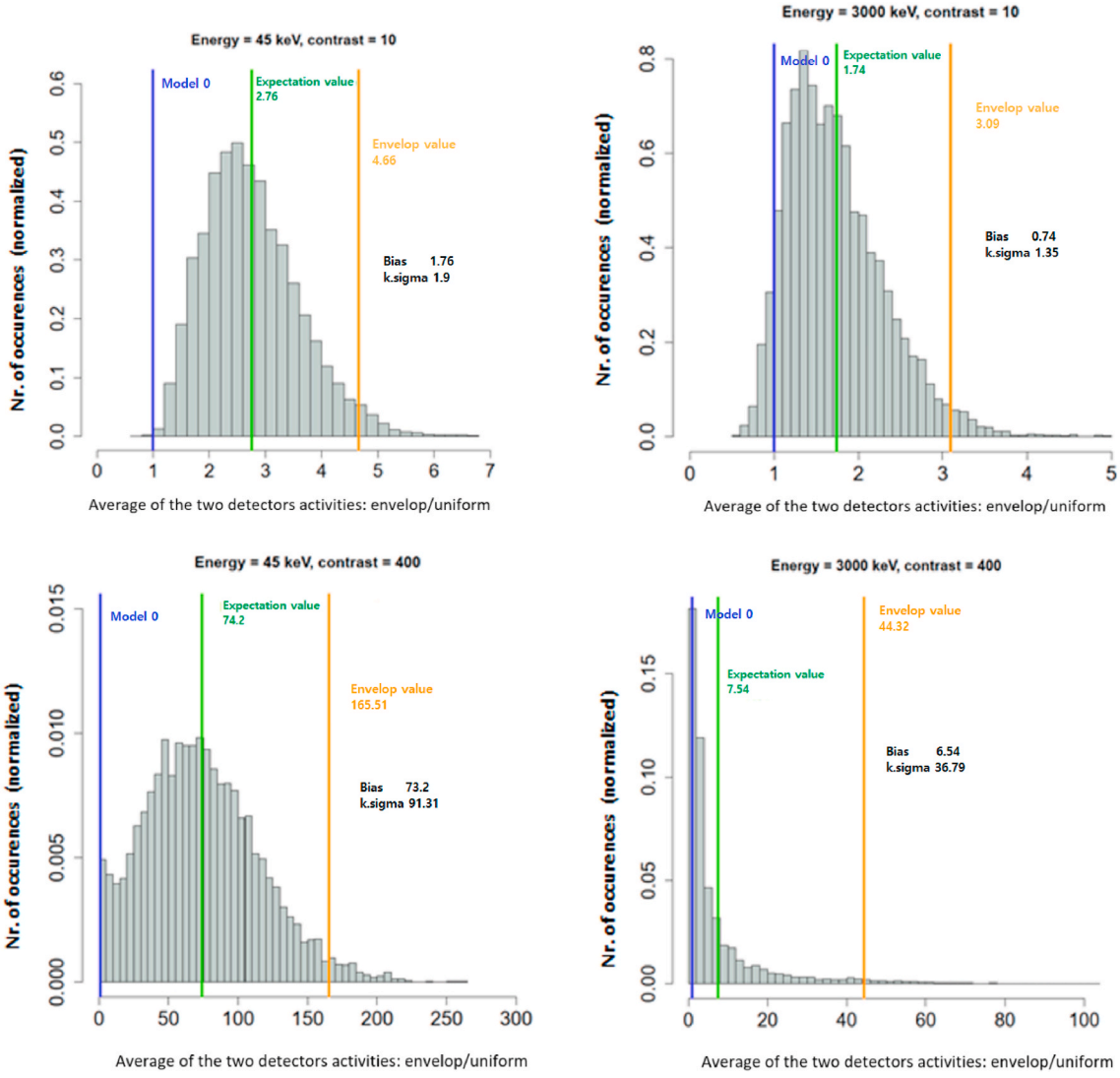

Fig. 12. Distribution of correction factors (1 + CF(E)) normalized for the uniform distribution (reference model, blue line). Optimized value is represented by the red line, expectation value is represented by the green line and characterizes the bias due to a heterogeneous source distribution ($\mathbb{B} = \boldsymbol{exp.value} - 1$). The envelop value is represented by the orange line and characterizes the random uncertainty due to a heterogeneous source distribution ($\boldsymbol{k\sigma} = \boldsymbol{pen.value} - \mathbb{B}$).

References

ANDRA, 2018. Guide d'enlèvement des déchets radioactifs. PPR. SP. ASNE. 18 0060. A. https://www.andra.fr/sites/default/files/2018-07/Andra-Guide_enlevement-2018C.pdf.

Bosko, A., Menaa, N., Spillane, T., Bronson, F., Venkataraman, R., Russ, W.R., Mueller, W., Nizhnik, V., 2011. Efficiency optimization employing random and smart search using multiple counts and line activity consistency benchmarks. In: Proceedings of WM2011 Conference, February 27-March 3.

Carrel, F., et al., Aug. 2014. Characterization of old nuclear waste packages coupling photon activation analysis and complementary non-destructive techniques. IEEE Trans. Nucl. Sci. 61 (4), 2137–2143.

J. Dumazert et al. Inverse Problem Approach for the underwater localization of Fukushima Daiichi fuel debris with fission chambers. Nuclear Instrumentation and Methods: A. Vol. 954, 161347.

Frosio, T., Menaa, N., Bertreix, P., Rimlinger, M., Theis, C., 2020. A novel technique for the optimization and reduction of gamma spectroscopy geometry uncertainties. Appl. Radiat. Isot. 156, 108953.

Frosio, T., Menaa, N., Duchemin, C., Riggaz, N., Theis, C., January 2020. A new gamma spectroscopy methodology based on probabilistic uncertainty estimation and conservative approach. Appl. Radiat. Isot. 155.

GUM, September 2008. Evaluation of Measurement Data. Supplement 1 of the Guide to the Expression of Uncertainty in Measurement. JCGM101:2008.

GUM, September 2008. Evaluation of Measurement Data. Guide to the Expression of Uncertainty in Measurement. JCGM100:2008.

IAEA, 2009. Determination and Use of Scaling Factors for Waste Characterization in Nuclear Power Plants. IAEA Nuclear Energy Series No. NW-T-1.18, Vienna.

IAEA Nuclear Energy Series. Determination and Use of Scaling Factors for Waste Characterization in Nuclear Power Plants. No NW-T-1.18.

ISO 21238, 2007. Nuclear Energy. Nuclear Fuel Technology. Scaling Factor Method to Determine the Radioactivity of Low- and Intermediate-Level Radioactive Waste Packages Generated at Nuclear Power Plants, Geneva, 2007.

Menaa, N., et al., 2011. Mathematical efficiency calibration with uncertain source geometries using smart optimization. In: 2nd International Conference on Advancements in Nuclear Instrumentation, Measurement Methods and Their Applications.

Spillane, T., Menaa, N., Atrashkevich, V., Bosko, A., Bronson, F., Nakazawa, D., Russ, W. R., Venkataraman, R., August 2010. An adaptive approach to mathematical efficiency calibration with uncertain source geometries. In: Proceedings of the American Nuclear Society Topical Meeting on Decommissioning, Decontamination and Reutilization.

Venkataraman, F., Bronson, V., Atrashkevich, M. Field, Young, B.M., 2003. Improved detector response characterization method in ISOCS and LabSOCS. In: Methods and Applications of Radioanalytical Chemistry (MARC VI) Conference.

Zaffora, B., 2017. Statistical Analysis for the Radiological Characterization of Radioactive Waste in Particle Accelerators, Paris: CERN-THESIS-2017-194. R.

Zaffora, B., Magistris, M., Frosio, T., Dyrcz, P., Theis, C., 2019. Radiological Characterization of VLLW Produced at High-Energy Particle Accelerators. WM2019 Conference. 3-7 March (Phoenix, USA).